

Metal-dielectric structures for high resolution imaging

Wang, Y. K.; Li, Dongdong; Zhang, Dao Hua; Yan, Changchun; Xu, Zhengji

2012

Li, D., Zhang, D. H., Yan, C. C., Wang, Y. K., & Xu, Z. (2012). Metal-dielectric structures for high resolution imaging. Proceedings of SPIE - The International Society for Optical Engineering, 8423.

<https://hdl.handle.net/10356/96962>

<https://doi.org/10.1117/12.923033>

© 2012 Society of Photo-Optical Instrumentation Engineers (SPIE). This paper was published in Proceedings of SPIE - The International Society for Optical Engineering and is made available as an electronic reprint (preprint) with permission of Society of Photo-Optical Instrumentation Engineers (SPIE). The paper can be found at the following official DOI: [<http://dx.doi.org/10.1117/12.923033>]. One print or electronic copy may be made for personal use only. Systematic or multiple reproduction, distribution to multiple locations via electronic or other means, duplication of any material in this paper for a fee or for commercial purposes, or modification of the content of the paper is prohibited and is subject to penalties under law.

Downloaded on 13 Mar 2024 17:10:58 SGT

Metal-dielectric structures for high resolution imaging

D. D. Li¹, D. H. Zhang^{1*}, C.C. Yan², Y. K. Wang¹ and Z. J. Xu¹

¹School of Electrical & Electronic Engineering, Nanyang Technological University, 639798 Singapore

²School of Physics and Electronic Engineering, Xuzhou Normal University, 221116 China

Corresponding email: edhzhang@ntu.edu.sg

ABSTRACT

Since Pendry's theoretical proposition of the perfect lens, extensive researches have been carried out in the field by a number of groups and various lenses and structures have been reported. In this article, we present and discuss light transmission in a vertical multilayered metal-dielectric structure and a metal chain array consisting of silver spheres with different diameters. For the incident wavelength of 660 nm, light can transmit a longer distance in the vertical multilayer structure due to low transmission loss. For the metal nanoparticle chain structure with an incident wavelength of 508 nm, the output light intensity can be greatly enhanced by adding a small sphere to the input end and output end, respectively as it is believed to enhance the coupling of the field into the structure and decoupling of the field from the structure, respectively.

Keywords: metamaterials, imaging, high transmission, low loss.

INTRODUCTION

Metamaterials, as one of the most promising artificially structured material for subwavelength imaging, have drawn a lot of attentions in recent years¹⁻¹². These metamaterial devices are usually made of metal-dielectric structures and they process unprecedented capability in manipulating electromagnetic waves in subwavelength scale. The topic was initiated by Sir Pendry, who first proposed the perfect lens and explained the concept of perfect imaging¹. As the perfect lens requires simultaneously negative permittivity and permeability, which is extremely hard to realize. Included in Pendry's proposal was a simplified near-field superlens that only requires negative permittivity. The superlens was first experimentally demonstrated by Fang and co-workers by a silver slab which is workable in ultraviolet (UV) range². Then several other groups reported similar lenses but made of different materials. Multilayered planar or curvature metal-dielectric structures were also proposed by several groups¹³⁻¹⁸. These layered metal-dielectric structures transfer the image through surface plasmons which is strongly affected by metal absorption. To construct such a lens with good performance, obtaining a low loss metal is essential. Thus most of the currently designed layered metal-dielectric lenses only work in the UV spectrum where noble metals have a relatively low loss. For real life applications, subwavelength imaging at visible frequencies is more desired, especially for biological applications where small living entities may possibly be killed under UV exposure. While the availability of low loss natural metals is very limited, researchers have to tailor with different designs to compensate the loss¹⁹⁻²². These new designs improved the performance of these devices by a certain extent, but there are still many challenges to overcome, such as narrow transmission spectrum and limited transfer distance.

The transmission loss of the layered metal-dielectric lens cannot be fully addressed by optimizing the design. Thus new structures should be explored in order to improve the imaging performance. Inspired by previous work, in this article, we

discuss several novel structures that are capable of subwavelength imaging, with lower transmission losses and better performance.

Subwavelength imaging with a vertically arranged metal-dielectric structure

For these layered metal-dielectric lenses, they are designed to work at the resonance surface plasmon frequency which is very suspicious to material absorption, resulting in low transmission. The problem can be avoided by designing the working frequency away from the resonance surface plasmon frequency. However, when the working frequency is shifted away from the resonance surface plasmon frequency, beam splitting occurs inside the layered metal-dielectric lenses. Thus, special design has to be employed in order to make the structure as a functional imaging device. Several groups have reported subwavelength resolution lenses by employing this idea²³⁻²⁵. In this article, we propose a vertically arranged metal-dielectric multilayer structure that is capable of high transmission. Figure 1 shows the cross-sectional diagram of the structure. It is made up of silver layers embedded in alumina covered by a chromium layer with two 50 nm width slits. We simulated the energy flow in the structure for the incidence with a wavelength of 660 nm as H-polarized plane wave. The permittivities of silver, chromium, and alumina used are extracted from Refs [26-28], respectively.

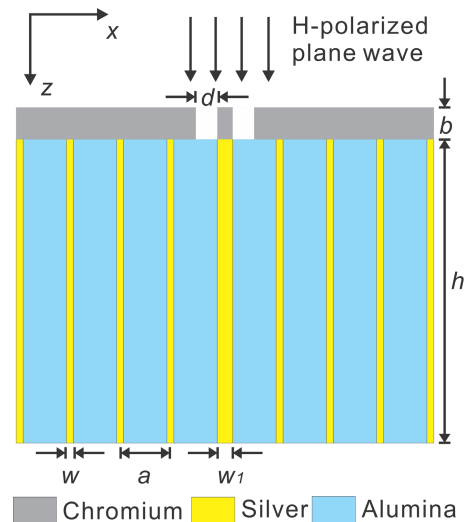


Figure 1. Cross-sectional schematic of the vertically arranged metal-dielectric lens. The geometric dimensions are $w = 16$ nm, $w_1 = 36$ nm, $b = 100$ nm, $h = 2000$ nm, and $a = 105$ nm. The slit width d is a variable.

Our simulations showed that, by controlling the thickness w_1 of the silver layer located in the middle of the structure, it is possible to project the majority of the light energy into one beam instead of two beam (normally beam splitting happens in such structure). Fig. 2(a) shows the energy flow distribution in the structure when w_1 is equal to or greater than 36 nm and only the slit on the left is illuminated. We also simulated the energy flow for slit widths of 30 nm and 10 nm and the same phenomena were observed. Figure 2 (b) shows the energy flow distributions inside the structure when both slit are illuminated. In this case, two beams can be observed. According to the analysis of Fig. 2(a), we can conclude that the left beam results from the left slit, while the right beam results from the right slit. Therefore, the structure can distinguish the two narrow slits with a spacing of only 36 nm which corresponds to a resolution of 0.055λ . More importantly, by moving the working frequency away from the resonance surface plasmon frequency, the transmission loss is reduced. Thus the beam can be transferred to a much longer distance, enable subwavelength imaging in the far-field. With the far-field subwavelength resolution arising from the metamaterial with two slits, sub-wavelength imaging of a broad luminescent object can be realized by scanning along the x direction over this object. For example, a scanning step length can be set to the summation of the widths of the two slits and of the chromium between them. The information from the two output beams can be recorded by a CCD camera during scanning. The recorded information is then input to a computer for image reconstruction and processing. The output beams recorded in the successive measurements need to be correctly registered in order to form the superresolved image of the object in the scanned direction. The metamaterial can be

translated in y or rotated with its rotation axis along z , to implement the same process and obtain the superresolved image in another direction.

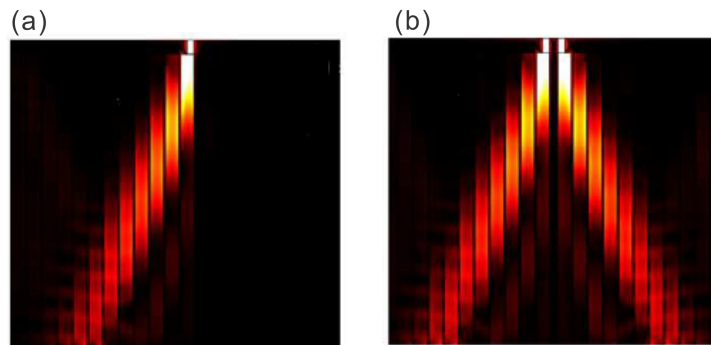


Figure 2. (a) Energy flow distribution in the vertical metal-dielectric multilayer structure when only the slit on the left is illuminated. (b) Energy flow distribution in the structure when both slits are illuminated.

Subwavelength imaging with an array of metallic nanoparticles

Other than the layered metal-dielectric structures, metallic nanoparticle chain-like structure were also proved to be a potential candidate for subwavelength imaging²⁹⁻³³. When the nanoparticles are spaced close each other, the strongly distance dependent near-field term in the expansion of the electric dipole interaction dominates, which leads to the excitation of electric-coupled plasmonic mode and coherent transportation of the energy at high efficiency^{34,35}. In addition, the dispersion properties of the metallic nanoparticles can be tuned by modifying the electric field interactions between the nanoparticles, which gives raise to extra degree of freedom over the control of the optical properties. Several groups have demonstrated subwavelength imaging using the chained metallic nanoparticle scheme³⁶⁻³⁸, with performance better than that of the layered lenses. In this article, we will discuss the effect of a small silver sphere/particle at input and output end of a chain consisting of a number of silver spheres/particles with greater diameters. It is found that by adding a smaller nanoparticle to the input and output of a nanoparticle chain, one can modify the decoupling and coupling efficiency of the field so as to enhance the transmission. Figure 3 shows the schematic of the structure made up of spherical silver nanoparticle array surrounded by air. Each chain in the array consists of three silver spheres with a diameter of 20 nm and two smaller silver spheres of diameter of 8 nm below and above the three big spheres. The space between the neighboring chains, d , is 40 nm.

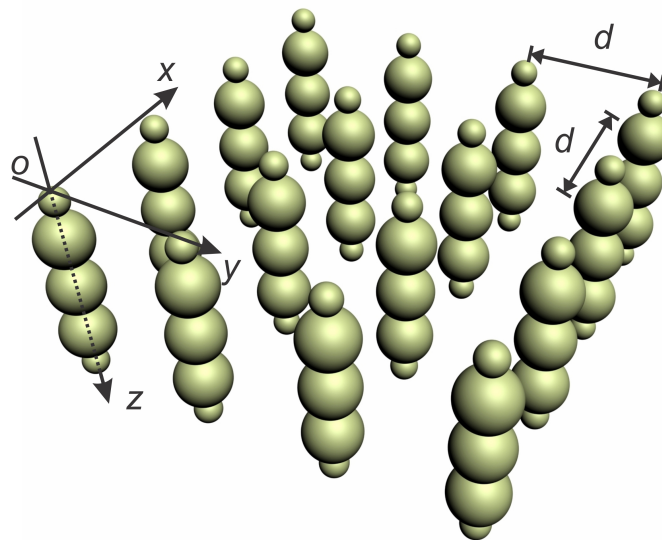


Figure 3. Schematic of a spherical silver nanoparticle array. The diameter of the large nanoparticles and small nanoparticles are 20 nm and 8 nm, respectively. The distance between the neighboring chains d is 40 nm.

For a dipole light source with a wavelength of $\lambda=508$ nm, we first studied the effect of the smaller silver nanoparticle on the decoupling efficiency. We simulated the output light intensities at the output surface of two chains, one of which consists of three silver nanoparticles of 20 nm diameter only and the other has one more silver nanoparticle with a diameter of 8 nm. The results are shown in Fig. 4. The dashed line in the figure represents the light intensity of the three nanoparticle chain at the output surface plane along the dot line shown in the chain image on the right of the figure while the solid line represents the light intensity of the chain with three big nanoparticles and one small nanoparticle at the output end. It is seen that the field intensity is enhanced about 12 times while the full width at half maximum (FWHM) is reduced to about 45% by simply adding a smaller nanoparticle at output. In the silver nanoparticle chains, the plasmonic wave usually travels along the surface of the nanoparticles. When a smaller particle is added at the output end, however, the plasmonic wave will be affected and it will propagate in a more convergent way, resulting in a higher intensity and narrower line width around the output surface of the chain. Obviously, this kind of reconstructed nanoparticle chain is advantageous for imaging applications.

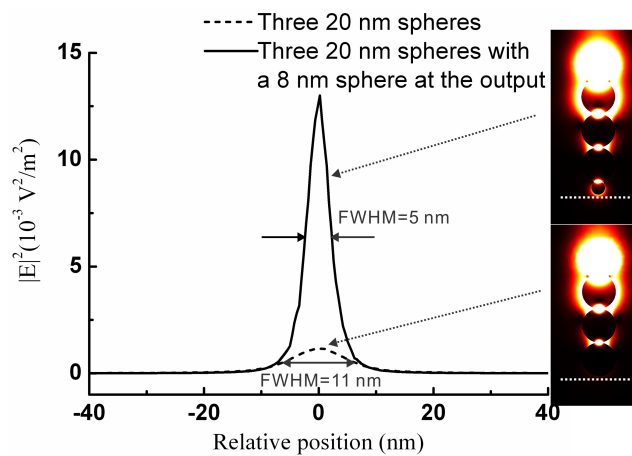


Figure 4. Field intensity distributions in the two silver nanoparticle chains consisting of three big nanoparticles only (dash curve) and three big and one small nanoparticles (solid curve). The diameters of the big and small nanoparticles are 20 nm and 8 nm, respectively.

Continuing with the above analysis, we now study the transmission efficiency of the nanoparticle chains with and without a small silver sphere in the input side of the chain. Fig. 5 shows the light intensity distribution at the output surface planes for the two cases. The dashed line represents the light intensity distribution measured at the output surface of the chain made of three identical nanoparticles with a diameter of 20 nm while the solid line represents the light intensity measured at the output surface of the chain which consists of three big silver particles of 20 nm diameters and a small nanoparticle of 8 nm diameter at the input side. It is found that better coupling of the energy from the light source to the silver nanoparticle chain can be achieved when a small silver sphere is added, resulting in field enhancement of about 3.3 times, which significantly improves the overall transmission.

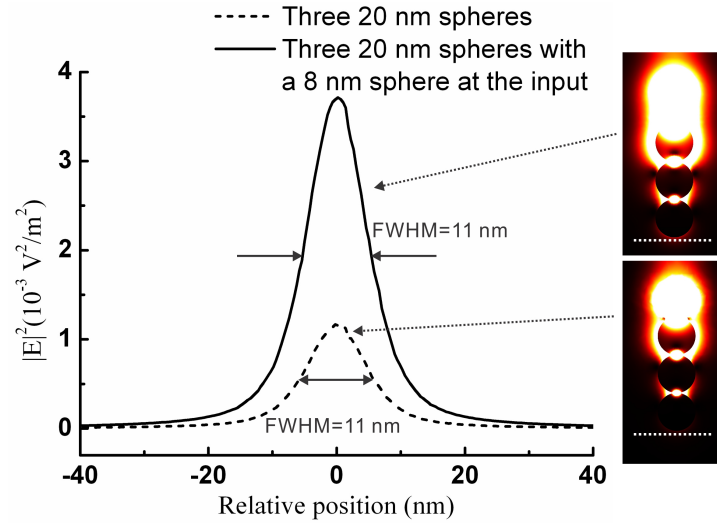


Figure 6. Field intensity distribution of the nanoparticle chains consist of three silver spheres of 20 nm diameter with/without a nanoparticle of 8 nm diameter at the input end.

Fig. 6 shows the light intensities (solid line) at output surface plane of the silver nanoparticle chain with a smaller one at both the input and output ends. Compared to the chain with a small nanoparticle at the output end only, the output field intensity is enhanced about 3 times while the FWHM is maintained almost the same.

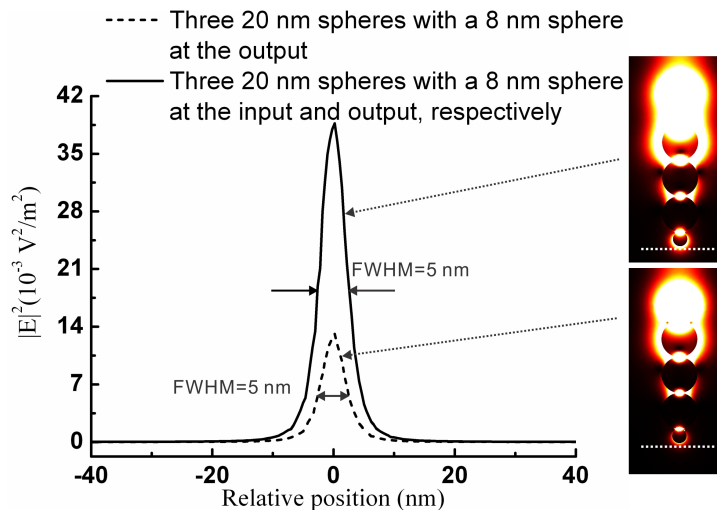


Figure 6. Field intensity (solid line) distribution of the nanoparticle chains consist of three 20 nm silver spheres and two small particles of 8 nm diameter at the input and output sides, respectively. The field distribution for the chain without the smaller particle at the input side (dashed line) is also included for comparison.

The above analysis shows that, the transmission efficiency of the nanoparticle chain structure is closely related to the coupling of the field into the structure and decoupling of the field from the structure. By adding a small sphere to the input end, the coupling efficiency can be enhanced, which benefits the overall transmission. Similarly, by adding a small sphere to the output end, the decoupling efficiency of the field energy from the nanoparticle chain to the output surface can be enhanced as well. In addition, the small nanoparticle at the output also provides a convergent pathway to concentrate the field, resulting further enhancement to the output light intensity.

CONCLUSION

In conclusion, we discussed both vertical multilayered structure and metal chain structure for imaging transmission. For the incident wavelength of 660 nm, the transmission loss in the vertical multilayer structure is decreased significantly and a long transmission distance of 2 μm is demonstrated. For the metal nanoparticle chain structure with the incidence of 508 nm, the transmission efficiency can be enhanced greatly by optimizing the coupling of the field into the structure and decoupling of the field from the structure. Our results show that by adding a small nanoparticle to the output end of the nanoparticle chain structure, the output light intensity can be enhanced 12 times and by adding another small nanoparticle to the input end of the nanoparticle chain, the output light intensity can be enhanced another 3 times.

ACKNOWLEDGEMENT

This project is supported by National Research Foundation (NRF-G-CRP 2007-01) and A*Star (092154009), Singapore.

REFERENCES

- [1] Pendry, J. B., "Negative refraction makes a perfect lens," *Phys. Rev. Lett.* 85, 3966–3969 (2000).
- [2] Fang, N. and Zhang, X., "Imaging properties of a metamaterial superlens," *Appl. Phys. Lett.* 82, 161–163 (2003).
- [3] Podolskiy, V. A., "Optimizing the superlens: manipulating geometry to enhance the resolution," *Appl. Phys. Lett.* 87, 231113 (2005).
- [4] Larkin, I. A. and Stockman, M. I., "Imperfect perfect lens," *Nano Lett.* 5, 339–343 (2005).
- [5] Liu, Z., Fang, N., Yen, T.-J. and Zhang, X., "Rapid growth of evanescent wave with a silver superlens," *Appl. Phys. Lett.* 83, 5184–5186 (2003).
- [6] Grbic, A. and Eleftheriades, G. V., "Overcoming the diffraction limit with a planar left-handed transmission-line lens," *Phys. Rev. Lett.* 92, 117403 (2004).
- [7] Lagarkov, A. N. and Kissel, V. N., "Near-perfect imaging in a focusing system based on a left-handed-material plate," *Phys. Rev. Lett.* 92, 077401 (2004).
- [8] Fang, N., Lee, H., Sun, C. and Zhang, X., "Sub-diffraction-limited optical imaging with a silver superlens," *Science* 308, 534–537 (2005).
- [9] Lee, H., Xiong, Y., Fang, N., Srituravanich, W., Durant, S., Ambati, M., Sun, C. and Zhang, X., "Realization of optical superlens imaging below the diffraction limit," *New J. Phys.* 7, 255 (2005).
- [10] Huang, Z. M., Xue, J. Q., Hou, Y., Chu, J. H. and Zhang, D. H., "Optical magnetic response from parallel plate metamaterials," *Phys. Rev. B* 74(19), 193105 (2006).
- [11] Wang, Y., Zhang, D. H., Wang, J., Yang, X., Li, D. and Xu, Z., "Waveguide devices with homogeneous complementary media," *Optics Letters*, 36, 3855–3857 (2011).
- [12] Melville, D. and Blaikie, R., "Super-resolution imaging through a planar silver layer," *Opt. Express* 13, 2127–2134 (2005).
- [13] Shi, L. H. and Gao L., "Subwavelength imaging from a multilayered structure containing interleaved nonspherical metal-dielectric composites," *Phys. Rev. B* 77, 195121 (2008).
- [14] Wood B., Pendry, J. B., and Tsai, D. P., "Directed subwavelength imaging using a layered metal-dielectric system," *Phys. Rev. B* 74, 115116 (2006).
- [15] Liu, Z., Lee, H., Xiong, Y., Sun, C. and Zhang, X., "Far-field optical hyperlens magnifying sub-diffraction-limited objects," *Science* 315, 1686 (2007).
- [16] Rho, J., Ye, Z., Xiong, Y., Yin, X., Liu, Z., Choi, H., Bartal, G. and Zhang, X., "Spherical hyperlens for two-dimensional sub-diffractional imaging at visible frequencies," *Nature Commun.* 1, 143 (2010).
- [17] Li, D., Zhang, D. H., Yan, C. and Wang, Y., "Two-dimensional subwavelength imaging from a hemispherical hyperlens," *Appl. Opt.* 50, 31 (2011).
- [18] Yan, C., Li, D. and Zhang, D. H., "Wedge-shaped metal-dielectric composite metamaterials for light control," *Metamaterials*, 4, 170–174 (2010).
- [19] Bloemer, M., D'Aguzzo, G., Mattiucci, N., Scalora, M. and Akozbek, N., "Broadband super-resolving lens with high transparency in the visible range," *Appl. Phys. Lett.* 90, 174113 (2007).

- [20] de Ceglia, D., Vincenti, M. A., Cappeddu, M. G., Centini, M., Akozbek, N., D'Orazio, A., Haus, J. W., Bloemer, M. J. and Scalora, M., "Tailoring metallodielectric structures for superresolution and superguiding applications in the visible and near-ir ranges," *Phys. Rev. A* 77, 033848 (2008).
- [21] Li, X., He, S. L. and Jin, Y., "Subwavelength focusing with a multilayered Fabry-Perot structure at optical frequencies," *Phys. Rev. B* 75, 045103 (2007).
- [22] Wang, Y., Zhang, D. H., Yan, C., Li, D. and Xu, Z., "Efficient and wide spectrum half-cylindrical hyperlens with symmetrical metal-dielectric structure," *Applied Physics A: Materials Science and Processing*, 1-4 (2011).
- [23] Yan, C., Zhang, D. H., Li, D. and Fiddy, M. A., "Metal-dielectric composites for beam splitting and far-field deep sub-wavelength resolution for visible wavelengths," *Opt. Express* 18, 14794 (2010).
- [24] Yan, C., Zhang, D. H., Li, D., Bian, H., Xu, Z. and Wang, Y., "Metal nanorod-based metamaterials for beam splitting and a subdiffraction-limited dark hollow light cone," *Journal of Optics*, 13, 8, 085102 (2011).
- [25] Zhao, Y., Nawaz, A. A., Lin, S. S., Hao, Q., Kiraly, B. and Huang, T. J., "Nanoscale super-resolution imaging via a metal-dielectric metamaterial lens system," *J. Phys. D: Appl. Phys.* 44, 415101 (2011).
- [26] Johnson, P. B. and Christy, R. W., "Optical constants of the noble metals," *Phys. Rev. B* 6(12), 4370-4379 (1972).
- [27] Palik, E. D., [Handbook of Optical Constants of Solids], Academic Press: Orlando, (1985).
- [28] Yao, J., Liu, Z. W., Liu, Y. M., Wang, Y., Sun, C., Bartal, G., Stacy, A. M. and Zhang, X., "Optical negative refraction in bulk metamaterials of nanowires," *Science* 321(5891), 930 (2008).
- [29] Quinten, M., Leitner, A., Krenn, J. R. and Aussenegg, F. R., "Electromagnetic energy transport via linear chains of silver nanoparticles," *Opt. Lett.* 23, 1331-1333 (1998).
- [30] Brongersma, M. L., Hartman, J. W. and Atwater, H. A., "Electromagnetic energy transfer and switching in nanoparticle chain-arrays below the diffraction limit," *Phys. Rev. B* 62, R16356 (2000).
- [31] Krenn, J. R., "Nanoparticle waveguides: watching energy transfer," *Nature Materials* 2, 210-211 (2003).
- [32] Maier, S., [Plasmonics: Fundamentals and Applications] Springer, Berlin, (2007).
- [33] Li, K., Stockman, M. and Bergman, D., "Self-similar chain of metal nanospheres as an efficient nanolens," *Phys. Rev. Lett.* 91, 227402 (2003).
- [34] Girard, C. and Quidant, R., "Near-field optical transmittance of metal particle chain waveguides," *Optics Express* 12, 6141-6146 (2004).
- [35] Alu, A., Belov, P. A. and Engheta, N., "Coupling and guided propagation along parallel chains of plasmonic nanoparticles," *New Journal of Physics* 13, 033026 (2011).
- [36] Huang, F. K., Chin, T. R. and Chan, C. T., "Analytical properties of the plasmon decay profile in a periodic metal-nanoparticle chain," *Opt. Lett.* 36, 2206-2208 (2011).
- [37] Noskov, Roman E., Belov, Pavel A. and Kivshar, Yuri S., "Subwavelength plasmonic kinks in arrays of metallic nanoparticles," *Opt. Express* 20, 2733-2739 (2012).
- [38] Kawata, S., Ono, A. and Verma, P., "Subwavelength colour imaging with a metallic nanolens," *Nature Photon.* 2, 438-442 (2008).